Springer

KSME

Journal of Mechanical Science and Technology 24 (3) (2010) 693~701
www.springerlink.com/content/1738-494x
DOI 10.1007/s12206-010-0201-2

A study on the development of a loading device using a photoelastic stress freezing method for the analysis of o-ring stress †

Jeong-Hwan Nam[1], Jai-Sug Hawong[1*], Kyo-Hyoung Kim[1], Liu-Yi[2], O-Sung Kwon[2] and Sung-Han Park[3]

[1]*Department of Mechanical Engineering, Yeungnam University, Gyeongsan, 712-749, Korea*
[2]*Graduate School of Mechanical Engineering, Yeungnam University, Gyeongsan, 712-749, Korea*
[3]*Agency for Defense Development, Daejeon,305-152, Korea*

(Manuscript Received July 9, 2009; Revised January 7, 2010; Accepted February 1, 2010)

Abstract

Typically, O-rings are used to prevent penetration of dust and alien substances from entering a cylinder during motion. Moreover, O-rings are used to create an air tight seal around a stationary shaft. The stresses developed in O-rings depend on the squeeze rate, gap between the external diameter of the groove and internal diameter of the cylinder as well as internal pressure. In application, the stress distributions in O-rings can be very complicated and are almost always studied through experiment. Photoelastic experiment has been applied to the study of 3-dimensional stress distributions in O-rings. The loading device used in photoelastic experiment is important. Its function is to apply a uniform squeeze rate and internal pressure on the O-ring and to allow uniform squeeze rate to be controlled. In this research, a loading device was developed to perform these functions. The validity of this loading device was confirmed through the stress distribution, the configuration change and the contact length of the O-ring. When the squeeze rate was constant, the upper and lower contact lengths of the deformed O-ring were almost equal. When internal pressure was applied to the O-ring, while under a uniform squeeze rate the upper contact length increases slightly with increase in internal pressure, while the lower contact length of the O-ring is constant with an increase in internal pressure.

Keywords: Stress freezing method; O-ring loading device; Contact length; Squeeze rate; Gap, O-ring

1. Introduction

Typically O-rings are used to either prevent the penetration of dust and alien substances from entering a cylinder during motion, or they are used to create an airtight seal around a stationary shaft. The airtight seal on a stationary O-ring is controlled by both the squeeze rate and the gap between the external diameter of the groove and the internal diameter of the cylinder. An O-ring with a uniform gap is generally under a uniform squeeze rate and internal pressure. Therefore, the stress distributions of an O-ring are very complicated and have been studied by many researchers. When the internal pressure of the rounded rectangular urethane ring are free, the compressive load in the radial direction of the rounded rectangular ring are applied and lateral one side of the rounded rectangular ring is restrained, the stress distributions of the rounded rectangular ring were analyzed by Antonio Strozzi [1] using photoelastic experiment and numerical method.

A. F. George and A. Strozzi [2] analyzed the stresses of a circular elastomer, which was laterally unrestrained, through experiment.

E. Dragoni [3, 4] developed a theoretical model of an O-ring based on the theory of linear elasticity. In his model, the lateral side of the O-ring is restrained by a gap with the varying width and internal pressures of the O-ring are free.

Using experimentation and numerical method, A. Strozzi and E. Dragoni analyzed the mechanical behavior of the O-ring and studied its contact stresses and contact lengths with variations in squeeze rates when the diameter of the O-ring's cross section and gap width were constant. They introduced the analyzing model on the lateral restrained effectiveness of O-ring.

Karaszkiewicz [5] used a finite element method to study the contact stresses of an O-ring both with and without internal pressures while the lateral side of the O-ring was unstrained.

Il Kwon Lee and Chung-Gun Kim [6] studied the extrusion behavior of an O-ring with internal pressures, interference among factors, different types of materials and the radius of

† This paper was recommended for publication in revised form by Associate Editor Jeong Sam Han

*Corresponding author. Tel.: +82 53 810 2445, Fax.: +82 53 810 4627
E-mail address: jshawong@ynu.ac.kr

the groove. Although there exist numerous studies on O-rings, there have been no studies performed on the analysis of stresses on O-rings under both uniform squeeze rate and internal pressure while the lateral side is restrained. The most important things in 3-dimensional photoelastic experiment are to make a model which is identical to the parts or is analogous to the parts to do experiment and to develop the loading device for the experiment. Therefore, the main aim of the present study is to develop an O-ring molding method and loading device that will apply uniform load and internal pressure to the O-ring either simultaneously or separately. The final aim of this research is to develop a 3-dimensional photoelastic experimental hybrid method for 3-dimensionl stress analysis of an O-ring under both a uniform squeeze rate and an internal pressure while the lateral side is restrained. The most important things in the three-dimensional photoelastic experiment are to make a model which is identical to the parts or is analogy to the parts to do experiment and to develop the loading device for experiment. Therefore, the main purpose of this research is to develop an O-ring molding method and loading device that will apply a uniform load and internal pressure to the O-ring either simultaneously or separately.

2. Basic theory

Fig. 1 shows the restrain conditions for O-ring assemblage.

Fig. 2 show the geometrical conditions of the deformed O-ring when O-ring is assembled.

a_u, a_l and a_f respectively indicate of upper contact length, lower contact length, front contact length of the O-ring when it is under a uniform squeeze rate or O-ring is under uniform squeeze rate and internal pressure. H is the height of the deformed O-ring under the above conditions. d is the diameter of cross-section.

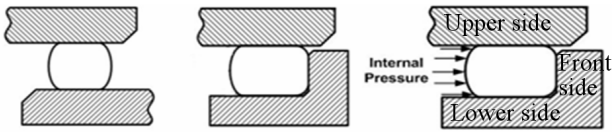

(a) Laterally unrestrained
(b) Lateral one side unrestrained
(c) Lateral one side restrained and internal pressure

Fig. 1. Restraint conditions for O-ring assembly.

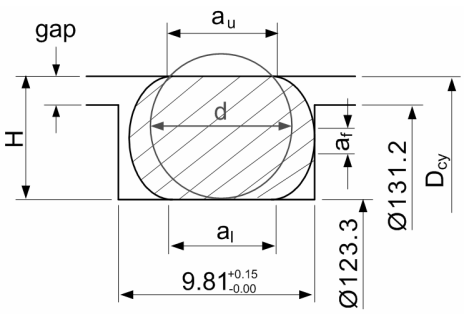

Fig. 2. Dimension of deformed O-ring.

The internal diameter of groove is $123.3^{+0.1}_{-0.0}$. The external diameter of groove is $131.2^{+0.03}_{-0.00}$. Width of groove is $9.81^{+0.13}_{-0.00}$. The gap is the difference between the external diameter of groove and the internal diameter of cylinder.

Eq. (1) is the relative equation between the total load applied to the O-ring, F, and the compressive deformation of O-ring, [7].

$$\frac{F}{\pi DdE} = \frac{g}{dE} = 1.25\left(\frac{x}{d}\right)^{\frac{3}{2}} \tag{1}$$

where a, F, g, d, D, E, x and x/d are indicate contact length, overall contact force, contact force per unit thickness, cross-sectional diameter of O-ring, mean diameter of O-ring, elastic modulus of O-ring, compressive deformation due to the contact force, and fractional compression of O-ring respectively.

Eq. (2) is experimental formula obtained using the hardening (vulcanite, hard) rubber.

$$\frac{F}{\pi DdE} = \frac{g}{dE} = 1.25\left(\frac{x}{d}\right)^{\frac{3}{2}} + 50\left(\frac{x}{d}\right)^{6} \tag{2}$$

The compressive load is obtained from Eq. (3)

$$F = \frac{\pi^2 a^2 DE}{6d} \tag{3}$$

Eq. (4) is obtained by substituting Eq. (3) into Eq. (2). Eq. (4) is the relative equation between the contact length of the O-ring and its cross-sectional diameter [8].

$$\frac{\pi}{6}\left(\frac{a}{d}\right)^2 = 1.25\left(\frac{x}{d}\right)^{\frac{3}{2}} + 50\left(\frac{x}{d}\right)^{6} \tag{4}$$

Eq. (5) is the experimental formula suggested by Lindley [8].

$$a = 2.4x \tag{5a}$$

$$\frac{a}{d} = 2.4\left(\frac{x}{d}\right) \tag{5b}$$

Eq. (5) is effective until the squeeze rate is 40%. Eq. (6) is the experimental formula suggested by Wendt [9].

$$\frac{a}{d} = 1.5\left(\frac{x}{d}\right)^{\frac{2}{3}} \tag{6}$$

Eq. (7) is the relative equation between the contact length of O-ring and its cross-sectional area. Eq. (7) suggested by Gorelik and Eeld'man [10] is similar to the relative equation between the diameter of the deformed sphere and the contact length suggested by Jagger and Walker [11].

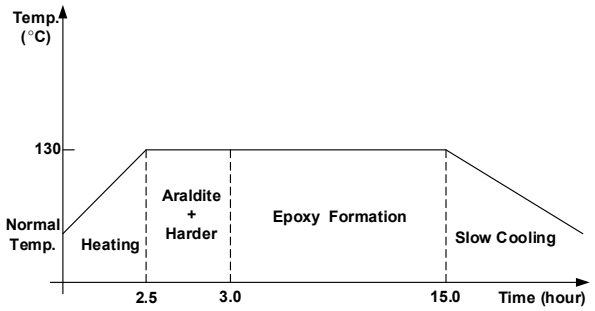

Fig. 3. Molding cycle in furnace.

$$\frac{a}{d} = 2\frac{x}{d} + 0.15, \quad 0.1 \le \frac{x}{d} \le 0.425 \tag{7a}$$

$$\frac{a}{d} = (2\frac{x}{d} + 0.15)^2, \quad 0.425 \le \frac{x}{d} \le 0.45 \tag{7b}$$

when the squeeze rate is less than 20%, Eq. (4), (5), (6) and (7) are still effective. However, when the squeeze rate is greater than 20%, the effectiveness of each equation varies.

3. Experimental and experimental method

3.1 O-ring molding process from epoxy resin

To analyze the stresses of the O-ring under arbitrary loads using a photoelastic experiment, the model specimen for the O-ring should be made from an epoxy resin, which is composed by mixing Araldite and hardener (HT 903) at a weight ratio of 10:3 (Araldite to hardener). The molding process to create an O-ring specimen is as follows:

(1) O-ring which is identical to actual O-ring should be made from iron or hard material.
(2) The iron template is placed at the center of the molding box.
(3) Silicon is poured into the molding box and allowed to set for 12 hours until it is completely solidified.
(4) The template is removed from molding box to create a silicon mold for the O-ring specimen.
(5) Araldite and hardener are weighted at a ratio of 10:3 respectively. They are then each placed into separate vessels and heated at 130℃ for 2 hours until they are completely liquefied.
(6) The hardener is pushed into the dissolved Araldite and mixed regularly 2 or 3 times at five minute interval and until they are completely dissolved. The mixture is then injected into the molding box and the bubbles are removed. The entire processes should be finished within 30 minutes after the hardener is put into the Araldite.
(7) After the bubbles are completely removed, the molding box with the Araldite and hardener should be heated for 12 hours according to the molding cycle shown in Fig. 3.

Table 1. Mechanical properties of epoxy resin.

Young's modulus (MPa)	15.6
Poisson's ratio	0.5
Hardening Temperature	120°C
$\alpha(m/kN)$	4.122

3.2 Experimental device

The photoelastic experimental device used in this research is a transparent photoelastic optical system. The mechanical properties of the epoxy resin under high temperature are shown in Table 1. The cross-sectional diameter is 6.98 ± 0.15 mm, the photoelastic sensitivity of the epoxy resin is 4.122 m/kN at 120℃. The elastic modulus of epoxy resin is 15.6 MPa. Slices are cut from the O-ring at 90° interval. The thickness of initial slice is about 2 mm. Slices are worn away using 100 to 2200 grit sandpaper until the thickness of slice is about 1 mm. The finished slices are put into a box containing a solution of α-Bromnaphtalene and fluid paraffin at a mixing ratio of 1:0.585 respectively. The box is put into a position where the specimen interacts with the transparent photoelastic experimental device and the isochromatic fringe patterns are recorded on a digital file.

The lengths in this research, i.e. cross sectional height of the O-ring (H), cross sectional width of the O-ring, contact length of the upper side (a_u), contact length of the lower side (a_l), contact length of the front side (a_f) and thickness (t) of the slice, were measured using a video microscope at 40 times magnification.

Fig. 4 is the experimental loading device that provided an internal pressure and uniform squeeze rate on the O-ring. Fig. 5 shows the parts of the loading device and the assembled loading device where a squeeze rate of 10% or 20% are applied.

The O-ring made from epoxy resin, the cylinder, and guide ring were heated at 120℃ for 40 minutes.

Then the O-ring, cylinder and guide ring were assembled in the stress freezing furnace. During this time the O-ring was in the region of glass transformation.

3.3 Three dimensional photoelastic experiment

3.3.1 Stress freezing method

When a polymer is heated over the point of glass transformation it behaves like rubber. This is also true for an O-ring made from epoxy resin, which is also a polymer. When a deformed polymer epoxy resin keeps its deformation, the internal stresses within the polymer are retained, this situation is called stress freezing. To facilitate stress freezing, a specimen made from epoxy is heated beyond the point of glass transformation and a load is applied for about one hour, then the specimen with the load is slowly cooled to room temperature. Although the load applied to the specimen is removed, the deformation of the O-ring is retained.

Birefringence is the splitting of one ray of light into two in

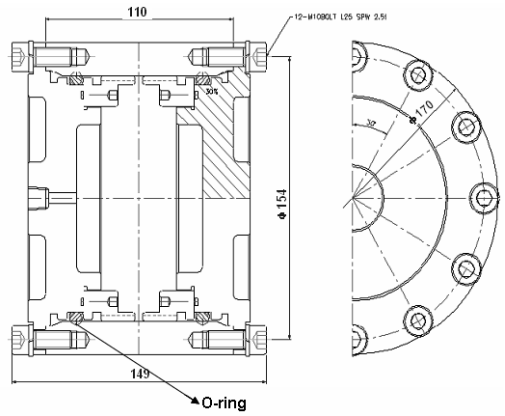

Fig. 4. Experimental loading device for O-ring under internal pressure and uniform squeeze.

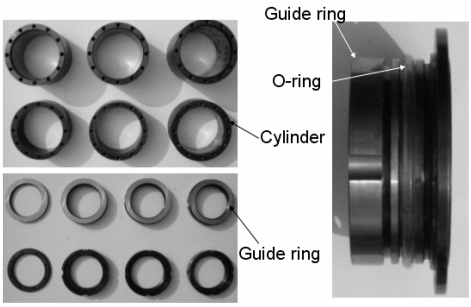

Fig. 5. Part of loading device for O-ring.

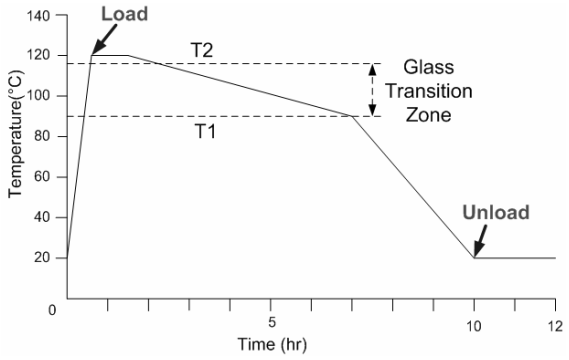

Fig. 6. Stress freezing cycle for epoxy resin.

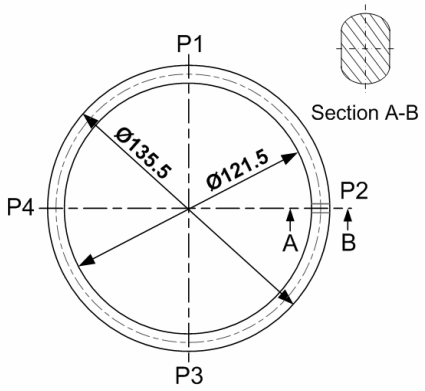

Fig. 7. Positions of sliced O-ring.

an anisotropic medium and is proportional to stress.

Therefore, birefringence is retained within the deformed polymer material containing photoelastic physical properties. When the three-dimensional model is cut into a slice, the birefringence is contained with in the slice. The stress components of the three-dimensional model are determined by cutting the specimen into slices using various methods then measuring the birefringence and combining the analysis of each slice. The situation of birefringence can be represented into an isochromatic fringe pattern by the photoelastic experimental device.

Stress analysis using an isochromatic fringe order is called a photoelastic stress freezing experiment. This method is mainly used the three-dimensional stress analysis of structures. Therefore, this method is called the three-dimensional photoelastic experiment. The stress analyzing procedures of this experimental method are as follows:

1) The material is selected for the three-dimensional photoelastic experiment.
2) The three-dimensional model is fabricated.
3) The loading device and specimen are both heated in the furnace.
4) The model is mounted to the loading device and loaded.
5) Stress freezing is conducted according to the stress freezing cycle.
6) A slice from the model is cut to analyze the stress freezing.
7) The data from slice is recorded and observed using the photoelastic experiment.
8) A stress analysis of the model is performed using the isochromatic fringe patterns.

3.3.2 Stress freezing cycle

The stress freezing cycle begins by heating the specimen and loading device beyond the point of glass transformation for 40 minutes in the furnace as shown in Fig. 6. The glass transformation point for epoxy resin is between 90℃ and 115℃.

The specimen was heated from 20℃ to 120℃ in the furnace and maintained at 120℃ for 1 hour. It was then cooled down from 120℃ to 90℃ at the rate of 5℃/h and then cooled further from 90℃ to 20℃ (room temperature) at the rate of 35℃/h. The slower the cooling velocity, the better the experimental conditions.

4. Experimental result and discussions

When the internal pressure to the O-ring was free, the squeeze rates were between 10% and 20% and the internal pressures were 0,98 MPa, 1.96 MPa, 2.94 MPa, and 3.92 MPa, the effectiveness of the loading device was confirmed through the deformation of O-ring's configuration and isochromatic fringe patterns.

4.1 When O-ring is free of internal pressure

4.1.1 10% squeeze rate

The O-ring was sliced every 90° to show the stress freezing. Fig. 7 shows the sliced positions of O-ring. The thicknesses of slice (a), (b), (c), and (d) in Fig. 8 are 1.07, 1.05, 0.96 and 1.02 mm respectively.

Fig. 8 shows the configuration of the deformed O-ring and the contact lengths of the upper side, lower side and front side at each position. Slice (a) was magnified 20 times and slices (b), (c) and (d) were magnified 40 times. The cross-sectional heights of the deformed O-ring at (a), (b), (c) and (d) were 6.35 mm, 6.43 mm, 6.38 mm and 6.43 mm respectively. The contact lengths of upper (lower front) side in the deformed O-ring are respectively 2.50 (2.37, 0.94) mm, 2.50 (2.31, 0.94) mm, 2.46 (2.31, 0.87) mm and 2.46 (2.31, 0.99) mm at position 1, position 2, position 3 and position 4 respectively.

The contact lengths of the upper side, lower side and front side were almost constant. This indicates that the loading device developed in this research is effective. Fig. 9 shows isochromatic fringe patterns of each slice under a 10% squeeze rate. The isochromatic fringe patterns and maximum fringe orders are completely identical to each other. This means that the same loading conditions can be applied to the O-ring using the loading device developed in this research.

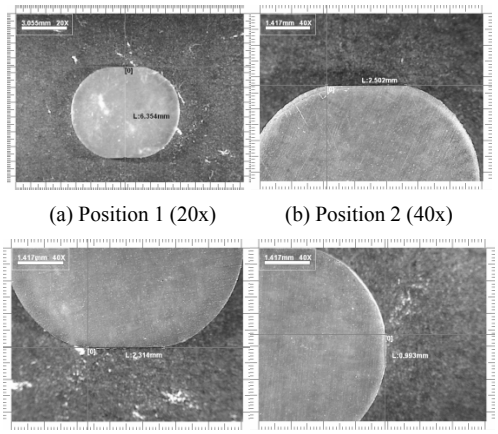

(a) Position 1 (20x) (b) Position 2 (40x)

(c) Position 3 (40x) (d) Position 4 (40x)

Fig. 8. Deformed configuration of O-ring under 10% squeeze rate.

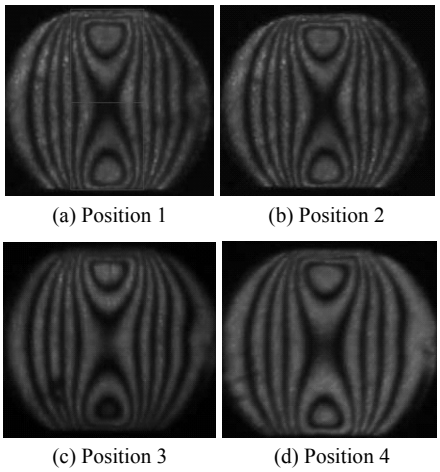

(a) Position 1 (b) Position 2

(c) Position 3 (d) Position 4

Fig. 9. Isochromatic fringe patterns of O-ring slice under 10% squeeze rate.

Position 1, 2, 3 and 4 show the isochromatic fringe patterns of slice 1, 2, 3 and 4 respectively.

Table 2 shows the contact length of the upper side, lower side, front side, the maximum fringe orders and the theoretical contact length of the deformed O-ring in each slice. Theoretical value means the theoretical contact length of upper side or lower side. The theoretical contact lengths of the upper side are equal to those of the lower side.

The experimental contact lengths of the upper side are slightly larger than those of the lower side. The theoretical values of the contact length were obtained from Eq. (4), (5), (6) and (7a).

The experimental contact length of the lower side is similar to the theoretical contact length of the upper side or lower side.

The results in Table 2 are largely due to the compressive forces that were transformed from the upper side of the O-ring to the lower side of the O-ring.

While the study called for a 10% squeeze rate, in practice only a 9% squeeze rate was actually applied to the specimen and was almost constant in each slice.

The above results show that the loading device developed in this research is very effective.

4.1.2 20% squeeze rate

When the squeeze rate is at 20%, the thicknesses of slices (a), (b), (c), and (d) in Fig. 10 are 1.03 mm, 1.05 mm, 0.95 mm and 0.89 mm respectively.

Fig. 10 shows the configuration of the deformed O-ring and the contact lengths of the upper side, lower side and front side at each position. The deformed O-ring was magnified 20 times and the contact lengths of each position were magnified 40 times. The cross-sectional heights of the deformed O-ring are 5.74 mm at each position. The contact lengths of the upper (lower, front) sides in the deformed O-ring are 4.00 (3.84, 1.52) mm, 3.91 (3.87, 1.51) mm at position 1, position 2, position 3 and position 4 respectively.

Table 2. Measured data of deformed O-ring under approximately 10% squeeze rate (unit : mm).

	Slice 1	Slice 2	Slice 3	Slice 4	Average value	values
a_u	2.50	2.50	2.46	2.46	2.48	
a_l	2.37	2.31	2.31	2.31	2.33	1.81*
a_f	0.94	0.94	0.87	0.99	0.93	1.55**
x/d	0.10	0.09	0.09	0.09	0.09	2.15***
H	6.35	6.43	6.38	6.43	6.40	2.35****
N_f	6	6	6	5	6	

N_f : fringe order

*, **, ***, **** : Values from experimental formula Eq. (4), (5), (6) and (7a) respectively.

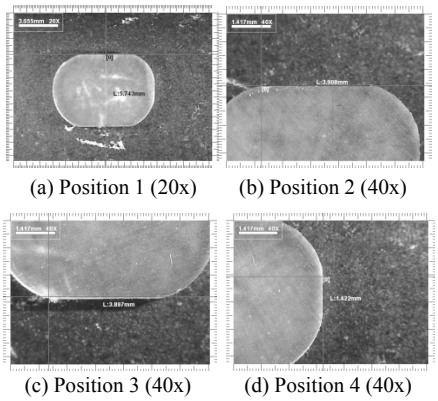

(a) Position 1 (20x) (b) Position 2 (40x)

(c) Position 3 (40x) (d) Position 4 (40x)

Fig. 10. Deformed configurations of O-ring under 20% squeeze rate.

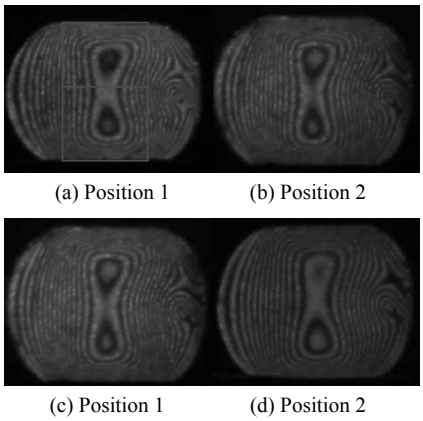

(a) Position 1 (b) Position 2

(c) Position 1 (d) Position 2

Fig. 11. Isochromatic fringe patterns of slices of O-ring under 20% squeeze rate.

The contact lengths of the upper side, lower side and front side are almost constant for each case. This indicates that the loading device developed in this research is effective and the revival properties are very high.

Fig. 11 shows the isochromatic fringe patterns of each O-ring slice under a 20% squeeze rate. The isochromatic fringe patterns are completely identical to each other irrespective of position. This means that the same loading conditions can be applied to the O-ring using the loading device developed in this research.

Table 3 shows the contact lengths of the upper side, lower side, front side, maximum fringe order and theoretical values of the contact length. The theoretical values of the contact length were calculated from Eqs. (4), (5), (6) and (7). The contact lengths of the upper side are slightly larger than those of the lower side. Those of the lower side are almost identical to the theoretical values. The contact lengths of the upper and lower sides are very similar to the theoretical values calculated from Eq. (7).

We intended to apply a squeeze rate of 20% to the O-ring, but actual the squeeze rate was approximately 18%. All squeeze rates were almost constant. These results mean that the loading device developed in this research is very effective for providing a uniform squeeze rate.

Table 3. Measured data of deformed O-ring under approximately 20% squeeze rate (unit : mm).

	Slice 1	Slice 2	Slice 3	Slice 4	Average value	Values
a_u	4.00	3.91	3.90	3.91	3.93	
a_l	3.84	3.83	3.90	3.90	3.97	3.09*
a_f	1.52	1.67	1.41	1.42	1.51	3.12**
x/d	0.18	0.18	0.18	0.18	0.18	3.42***
H	5.74	5.74	5.74	5.74	5.74	3.66****
N_f	12	12	12	11	12	

N_f: fringe order

*, **, ***, **** : Values from experimental formula Eq. (4), (5), (6) and (7a) respectively.

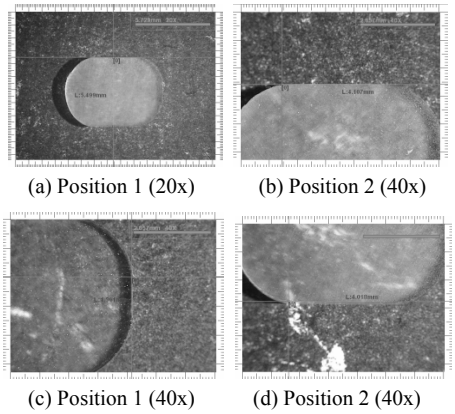

(a) Position 1 (20x) (b) Position 2 (40x)

(c) Position 1 (40x) (d) Position 2 (40x)

Fig. 12. Deformed configuration of the stress frozen O-ring under 22% squeeze rate with internal pressure (0.98 MPa).

4.2 20% squeeze rate and variable internal pressure

When squeeze rate was set at 20% and the internal pressures varied at 0.98 MPa, 1.96 MPa, 2.94 MPa and 3.92 MPa; the following metrics were analyzed: the configurations of the deformed O-ring; the contact lengths of the upper, lower and front sides; and the isochromatic fringe patterns of each point.

In this paper, the representative experimental results were evaluated. When squeeze rate is 22% and internal pressure is 1.96 MPa, the thicknesses at each position are 1.02 mm, 0.98 mm, 0.95 mm and 1.08 mm. When squeeze rate is 23% and internal pressure is 2.94 MPa, the thicknesses at each position are 0.96 mm, 0.94 mm, 0.95 mm and 0.89 mm. When squeeze rate is 22% and internal pressure is 3.92 MPa, the thicknesses at each position are 0.98 mm, 0.92 mm, 0.95 mm and 0.89 mm.

Fig. 12(a), (b), (c) and (d) show the configuration of the deformed O-ring, the contact length of upper side, the contact length of the lower side and the contact length of the front side respectively, when the squeeze rate is 22% and the internal pressure is 0.98 MPa.

Fig. 13(a), (b), (c) and (d) show the configuration of the stress frozen O-ring, the contact length of upper side, the contact length of the lower side and the contact length of front side respectively, when squeeze rate is 22% and internal pres-

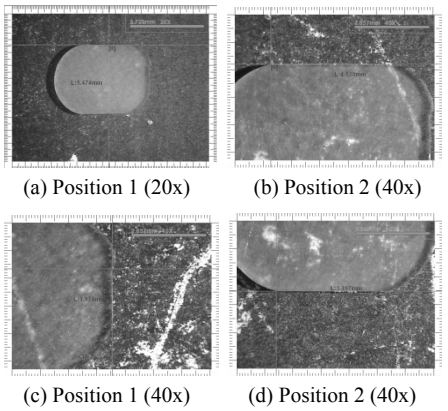

(a) Position 1 (20x) (b) Position 2 (40x)

(c) Position 1 (40x) (d) Position 2 (40x)

Fig. 13. Deformed configuration of the stress frozen O-ring under 20% squeeze rate with internal pressure (3.92 MPa).

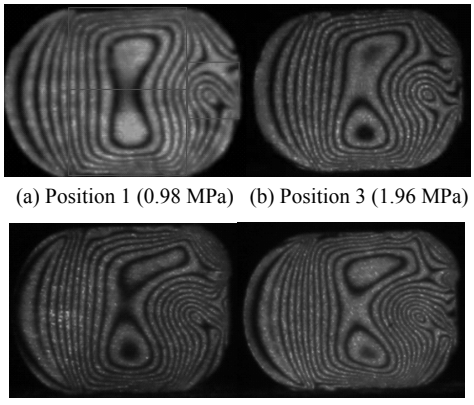

(a) Position 1 (0.98 MPa) (b) Position 3 (1.96 MPa)

(c) Position 5 (2.94 MPa) (d) Position 7 (3.92 MPa)

Fig. 14. Isochromatic fringe patterns of slices of the stress frozen O-ring under about 22% squeeze with internal pressure.

sure is 3.92 MPa.

Fig. 14(a), (b), (c) and (d) show the representative isochromatic fringe patterns when the internal pressures are 0.98 MPa, 1.96 MPa, 2.94 MPa and 3.92 MPa respectively. When the internal pressure is constant, the maximum fringe orders of each position are also constant.

Table 4 through 7 show the contact lengths of the upper side, lower and front sides, average values of the contact length in each side, theoretical values and the maximum fringe orders when the internal pressures are 0.98 MPa, 1.96 MPa, 2.94 MPa and 3.92 MPa respectively.

The contact length of each side is constant in all cases and the contact length of the upper side is similar to the value from experimental formula Eq. (7). The contact lengths of the lower side are similar to the theoretical values calculated from Eqs. (6), (7), (5) and (6) when the internal pressures are 0.98 MPa, 1.96 MPa, 2.94 MPa and 3.92 MPa respectively.

When the O-ring is under a uniform squeeze rate and internal pressures, the contact length of lower side is very similar to the value from experimental formula Eq. (6).

When the squeeze rate is 22% and the internal pressures are 0.98 MPa, 1.96 MPa, 2.94 MPa, and 3.92 MPa; the contact

Table 4. Measured data of deformed O-ring under approximately 22% squeeze rate and 0.98 Mpa (unit : mm).

	Slice 1	Slice 2	Slice 3	Slice 4	Average value	Values
a_u	4.07	4.11	4.16	4.04	4.10	
a_l	3.97	3.99	4.02	3.81	3.95	3.62*
a_f	1.58	1.59	1.53	1.50	1.55	3.78**
x/d	0.23	0.23	0.22	0.22	0.22	3.89***
H	5.43	5.43	5.52	5.50	5.47	4.20****
N_f	8	8	8	8	8	

N_f : fringe order

*, **, ***, **** : Values from experimental formula Eq. (4), (5), (6) and Eq. (7a) respectively.

Table 5. Measured data of deformed O-ring under approximately 20% squeeze rate and 1.96 Mpa (unit : mm).

	Slice 1	Slice 2	Slice 3	Slice 4	Average value	Values
a_u	4.31	4.35	4.31	4.37	4.33	
a_l	3.69	3.61	3.70	3.60	3.65	3.62*
a_f	1.58	1.66	1.61	1.64	1.62	3.78**
x/d	0.23	0.23	0.22	0.22	0.22	3.89***
H	5.43	5.43	5.52	5.50	5.47	4.20****
N_f	9	9	9	9	9	

N_f : fringe order

*, **, ***, **** : Values from experimental formula Eq. (4), (5), (6) and (7a) respectively.

Table 6. Measured data of deformed O-ring under approximately 20% squeeze rate and 2.94 Mpa (unit : mm).

	Slice 1	Slice 2	Slice 3	Slice 4	Average value	Values
a_u	4.45	4.49	4.53	4.51	4.49	
a_l	3.88	3.85	3.82	3.79	3.82	3.66*
a_f	1.73	1.70	1.73	1.73	1.72	3.82**
x/d	0.23	0.23	0.23	0.23	0.23	3.92***
H	5.45	5.45	5.45	5.45	5.45	4.24****
N_f	10	10	10	9	10	

N_f : fringe order

*, **, ***, **** : Values from experimental formula Eq. (4), (5), (6) and (7a) respectively.

lengths of the upper side are greater than those of lower side by 3.6%, 16%, 14.71% and 14.17% respectively.

When the internal pressures are greater than 1.96 MPa, the contact lengths of the upper side are greater than those of the lower side by constant quantity.

The maximum fringe order for each case are constant at each position as shown in Tables 4 through 7. From these results it is known that the revival characteristics of the loading device developed in this research is very high.

Fig. 15 shows the relationship between the internal pressures and contact lengths.

The following graph shows the average contact lengths of

Table 7. Measured data of deformed O-ring under approximately 20% squeeze rate and 3.92 Mpa (unit : mm).

	Slice 1	Slice 2	Slice 3	Slice 4	Average value	Values
a_u	4.42	4.53	4.57	4.59	4.55	
a_l	3.89	3.91	3.90	3.94	3.91	3.61*
a_f	1.96	2.07	1.97	1.97	1.99	3.76**
x/d	0.22	0.22	0.22	0.22	0.22	3.88***
H	5.47	5.47	5.47	5.47	5.47	4.19****
N_f	10	10	10	10	10	

N_f: fringe order
*, **, ***, **** : Values from experimental formula Eq. (4), Eq. (5), Eq. (6) and Eq. (7a) respectively.

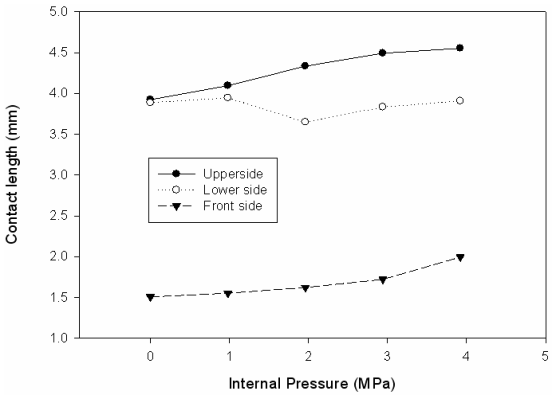

Fig. 15. Contact length with internal pressure.

the upper, lower and front sides.

Diamond, square, and triangle symbols indicate experimental contact length experimental value of upper side, lower side and front side respectively.

As shown in Fig. 15, the average contact lengths of the upper side and the front side are proportional to the internal pressures, but the average contact lengths of lower side are almost constant with for all internal pressures. When the internal pressure is less than 0.98 MPa, the average contact length of upper side are slightly larger than the average contact length of lower side.

When the internal pressure is between 1.96 and 3.92 MPa, the average contact length of the upper side is slightly larger than the average contact length of lower side. This phenomenon is due to the fact that the O-ring was squeezed from the top to the bottom inside the O-ring assembly.

Fig. 16 shows the average height of the deformed O-ring as a function of internal pressure.

As shown in Fig. 16, the average cross-sectional height of the deformed O-ring is almost constant for all internal pressures. This is the result of a change in internal pressure and a constant squeeze rate. Therefore, it is known that the loading device developed in this research is very effective in conditions where the internal pressure is changed and squeeze rate is constant. When the internal pressures are 0 MPa, 0.98 MPa, 1.96 MPa, 2.94 MPa, and 3.92 MPa, the average contact

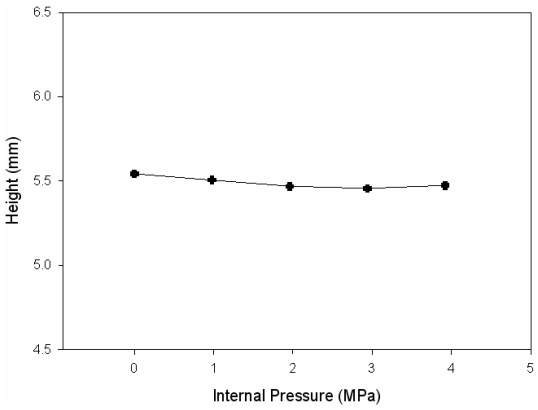

Fig. 16. Relationship between internal pressure and the height for O-ring under about 20% squeeze rate.

lengths of the upper side (lower side, front side) are 3.923 (3.886, 1.506) mm, 4.096 (3.946, 1.506) mm, 4.334 (3.648, 1.622) mm, 4.49 (3.833, 1.721) mm and 4.553 (3.908, 1.721) mm respectively.

When the internal pressures are 0 MPa, 0.98 MPa, 1.96 MPa, 2.94 MPa and 3.92 MPa, the cross-sectional average heights of the deformed O-ring are 5.543 mm, 5.505 mm, 5.469 mm, 5.456 mm and 5.474 mm respectively, this shows that the cross-sectional height is independent of the internal pressure. When the squeeze rate is constant, the cross-sectional height of the deformed O-ring should be constant. Therefore, the evidence shows that the loading device developed in this research is very effective for the case in which the loading device produces a uniform squeeze rate on the O-ring.

5. Conclusions

The following conclusions are obtained from the above experiments and discussions:

(1) The loading device developed in this research is effective for the case in which it produces a uniform squeeze rate and a uniform load.
(2) With the internal pressure between 0 MPa and 3.92 MPa and a constant squeeze rate, the cross-sectional height of the deformed O-ring is constant irrespective of internal pressure.
(3) When the squeeze rate is constant and the internal pressure is less than 2.94 MPa, the contact lengths of the upper or lower side are proportional to the internal pressure. When the internal pressure is greater than 2.94 MPa, the contact length of the upper or lower side are constant, but the contact lengths of the front side are only slightly proportional to the internal pressure.
(4) When O-ring is assembled and the internal pressures are 0.98 MPa, 1.96 MPa, 2.94 MPa and 3.92 MPa, the contact lengths of upper side are greater than those of lower side by 3.6%, 16%, 14.71% and 14.17% respectively. That is, when the internal pressures are greater

than 1.96 MPa, the increments between the contact lengths of the upper side and those of the lower side are constant.

(5) When only a uniform squeeze rate is applied to the O-ring, the contact length of the lower side is similar to the value from experimental formula calculated from Eq. (7a) than those of the upper side. Eq. (7) can be used to calculate the contact lengths of the deformed O-ring when only a uniform squeeze rate is applied.

(6) When a uniform squeeze rate and an internal pressure are applied to the O-ring, the contact lengths of upper side are very similar to the value from experimental formula from Eq. (7). When the internal pressures are 0.98 MPa, 1.96 MPa, 2.94 MPa and 3.92 MPa, the contact lengths of the lower side are very similar the values from experimental formula Eq. (4), (5), (6) and (7a) respectively. In general, the values from experimental formula calculated from Eq. (6) are very similar to these experimental values for any case.

References

[1] A. Strozzi, Static Stresses in an Unpressurized, rounded, rectangular, elastometric seal, Asle Transactions, 29 (4) (1986) 558-564.

[2] A. F George, A. Strozzi and J. I. Rich, Stress fields in a compressed unconstrained elastomeric O-ring seal and a co MParison of computer predictions with experimental results, Tribol. Int., 20 (1987) 237-247.

[3] E. Dragoni and A. Strozzi, Theoretical analysis of an unpressurized elastomeric O-ring seal into a rectangular groove, Elsevier Sequoia, Wear, 130 (1989) 41-51.

[4] E. Dragoni and A. Strozzi, Analysis of an unpressurized, laterally restrained, elastomeric O-ring seal, Journal of Tribology, 110 (1988) 193-200.

[5] A. Karaszkiewicz, Geometry and contact pressure of an O-ring mounted in a seal groove, Ind. Eng. Chem. Res. 29, (1990) 2134-2137.

[6] I. K. Lee and C. K. Kim, Numerical simulations on the O-ring extrusion in automotive engines, Journal of the KSTLE, 15 (4) (1999) 297-303.

[7] D. B. Lindley, Load compression relationship of rubber units, J. Strain Analysis, (1996) 190-195.

[8] D. B. Lindley, Compression characteristics of laterally-unstrained rubber O-rings, J. of IRI, 1, (1967) 209-213.

[9] A. F. George, A. Strozzi and J.I. Rich, Stress fields in a compressed unconstrained elastomeric O-ring seal and a co MParison of computer predictions with experimental results", Tribol. Int., 20 (5), (1987) 237-247.

[10] B. M. Gorelik and G. I. Feld'man, Study of stresses in a flat section of a rubber sealing ring of circular transverse section, Soviet Rubber Technology, (4) (1965) 27-31.

[11] E. T. Jagger and P. S. Walker, Further Studies of the lubrication of synthetic rubber rotary shaft seals, Proc. Inst. Mech. Engrs, 181 Pt I (9), (1966-1967) 191-204.

Jeong-hwan Nam received a B.S. degree in Mechanical Engineering from Yeungnam University in 1986. Then he received his M.S. degree and Ph.D. degree from Yeungnam University in Korea in 1996 and from Saitama Institute of Technology in Japan in 2005, respectively. Dr. Nam is currently a Researcher at the school of Mechanical Engineering at Yeungnam University, in Gyeongsan city, Korea. Dr. Nam's research interests are the areas of mechanical design, stress analysis and experimental mechanics for stress analysis etc.

Jai-Sug Hawong received a B.S. degree in Mechanical Engineering from Yeungnam University in 1974.
Then he received his M.S. degree and Ph.D. degree from Yeungnam University in Korea in 1976 and from Kanto Gakuin University in Japan in 1990, respectively. Prof. Hawong is currently a professor at the school of Mechanical Engineering at Yeungnam University, in Gyeongsan city, Korea. He is currently serving as an president of Korea Society Mechanical Engineering. Prof. Hawong's research interests are the areas of static and dynamic fracture mechanics, stress analysis, experimental mechanics for stress analysis and composite material etc.